NASA TECHNICAL NOTE

NASA TN D-3231

NASA TN D-3231

EXPERIMENTAL DATA ON PUMPING OF MERCURY ION BEAMS BY LIQUID-NITROGEN-COOLED CONDENSERS

by Edward A. Maslowski

Lewis Research Center
Cleveland, Ohio

NATIONAL AERONAUTICS AND SPACE ADMINISTRATION • WASHINGTON, D. C. • JANUARY 1966

NASA TN D-3231

EXPERIMENTAL DATA ON PUMPING OF MERCURY ION BEAMS BY LIQUID-NITROGEN-COOLED CONDENSERS

By Edward A. Maslowski

Lewis Research Center
Cleveland, Ohio

NATIONAL AERONAUTICS AND SPACE ADMINISTRATION

For sale by the Clearinghouse for Federal Scientific and Technical Information
Springfield, Virginia 22151 – Price $1.00

EXPERIMENTAL DATA ON PUMPING OF MERCURY ION BEAMS BY LIQUID-NITROGEN-COOLED CONDENSERS

by Edward A. Maslowski

Lewis Research Center

SUMMARY

A program was conducted to evaluate the performance of liquid-nitrogen-cooled condensers in pumping the exhaust of mercury ion thrustors. Tests were conducted with two different condensers. One of the condensers was a smooth cylinder having a total surface area of 3.8 square meters, and the other condenser was of honeycomb type of construction and had a total surface area of 62.9 square meters. Two targets, having apex angles of 32° and 148°, respectively, were used with each condenser. Ion beam current ranged from 10 to 200 milliamperes and accelerating potential from 2.0 to 6.0 kilovolts.

The results were evaluated on the basis of a performance factor F^* which is a function of the condenser accommodation and sticking coefficients. A mean value of F^* of 0.75 was determined in this study. A visual observation of mercury distribution patterns showed that the ratio of effective pumping area to actual geometric area was 0.4 for the smooth condenser and 0.1 for the honeycomb condenser. This study showed no significant difference in the effect of the two targets.

INTRODUCTION

Diffusion pumps prove to be limited in the ability to remove relatively large mass efflux at low pressures, as is the case when ion thrustors are operated in a vacuum facility. Cryopumps prove to be simple and effective means of removing large quantities of condensable gases at low pressures.

A cryopump of a given condensing area is generally as effective in removing condensable gases as a diffusion pump of the same throat area. By the use of geometric configurations such as fins or cells, considerable cryopump surface area can be incorporated in a vacuum system. However, mutual shielding by parts of a complex geometry decreases the pumping effectiveness of the total area. This effect is most pronounced in the case of an ion thrustor, which produces an energetic molecular beam.

A cryopump for rocket exhausts consists of two elements, a target and a cryogenically cooled condenser. In theory, the exhaust beam strikes the target and loses a substantial part of its energy and is then deflected to the condenser. The condensation is effected when each molecule of the impinging gas loses sufficient energy to stick to the condenser surface. During the process, a certain amount of noncondensables is released by the beam striking adsorbed layers of gas. These are removed by a diffusion pump.

The following relation, which gives the pressure rise due to the impingement of a molecular beam on a condensing surface, is available from reference 1:

$$\Delta p = \frac{2Nmv}{3S}\left[1 + (1 - f)(1 - a)^{1/2}\right](1 - f)(1 - a)^{1/2} \tag{1}$$

(All symbols are defined on p. 3.)

Let

$$F_{(a,\,f)} = \left[1 + (1 - f)(1 - a)^{1/2}\right](1 - f)(1 - a)^{1/2}$$

by substitution of the appropriate ion engine parameters,

$$N = \frac{J}{e}$$

$$v = \sqrt{\frac{2e}{m}V}$$

this equation becomes

$$F_{(a,\,f)} = 141.3\sqrt{\frac{e}{m}}\,\frac{S\,\Delta p}{J\sqrt{V}} \tag{2}$$

for Δp in torr. This has been carried out in somewhat more detail in reference 2, in which the equation is finally presented in the form

$$F^* = 141.3\sqrt{\frac{e}{m}}\,\frac{S\,\Delta p^*}{J\sqrt{V}} \tag{3}$$

where Δp^* indicates the pressure rise as read on the gage in recognition of the fact that the gage pressure reading may differ from the true pressure. Then F^* is the factor

$F_{(a, f)}$ based on this uncorrected pressure reading.

It should be noted that the factor $F_{(a, f)}$ involves values of sticking factor f and thermal accommodation coefficient a which could, in theory, be obtained separately and from which $F_{(a, f)}$ could be computed. However, these factors are empirical and prove to be difficult to obtain. Values for these factors are strongly dependent not only on surface material, but on surface finish and condition, including cleanliness, to an extent that precludes the application of values available from literature to a practical working condenser. An extensive treatment of this subject can be found in reference 3. The usefulness of F^* lies in the fact that it combines the sticking factor and the accommodation coefficient in a single factor which may be experimentally determined for a particular condenser.

A previous investigation (ref. 2) was performed on the design of cryogenic condensers for mercury ion thrustor beams. The condensers tested were 32 by 32 centimeters square and 46 centimeters in length and 16 by 16 centimeters square by 46 centimeters long. The interior of these were either plain walled or fitted with fins or honeycomb to yield surface areas ranging from 0.27 to 5.76 square meters. In the present study condensers of larger major dimensions (80 cm i.d. and 152 cm in length) and geometric area (3.8 and 62.9 m^2) were tested to extend the range of available data.

SYMBOLS

a	accommodation coefficient
e	electronic charge, C
F^*	cryopump performance factor based on Δp^*
$F_{(a, f)}$	cryopump performance factor
f	sticking factor
J	current, A
m	mass of molecule, kg
N	number of molecules per unit time
Δp	pressure rise, torr
Δp^*	pressure rise indicated by ionization gage
S	area, m^2
V	potential difference, volts
v	molecular beam velocity, m/sec

APPARATUS AND PROCEDURE

The vacuum system used consisted of a 5-foot-diameter by 6-foot-high mild steel tank. The interior of the tank was coated with an alkyd resin. The pumping system consisted of a 32-inch oil-diffusion pump with a water-cooled baffle. The baffled diffusion pump had a measured pumping speed of 10 000 liters per second.

Two condensers were tested. One condenser was a smooth copper cylinder with an inside diameter of 80 centimeters and 152 centimeters high. The second condenser was constructed by welding 15-centimeter-long, 3.8 by 3.8-centimeter-square ducts to vertical cooling tubes, as shown in figure 1. The latter condenser is, for convenience, referred to as a honeycomb condenser in this report. Its appearance is very similar to that of a honeycomb, although the cell is square instead of the hexagonal shape characteristic of a true honeycomb. The inside diameter of the honeycomb condenser was 80 centimeters, the outside diameter 112, and the height 152. The geometric surface area of the smooth condenser was 3.8 square meters, and that of the honeycomb condenser was 62.9 square meters. The geometric surface area is the area as seen from within the condenser. In the case of the smooth condenser, this is the inner surface of the cylinder. In the case of the honeycomb condenser, this is the total inner and outer surface area of the ducts and one-half of the area of the cooling tubes.

The ion beam source used was a 20-centimeter-diameter Kaufman thrustor. A complete description of this type of engine can be found in reference 4. Three sizes of propellant flow control orifices were used with this thrustor, having diameters of 0.257, 0.358, and 0.460 centimeter, respectively, from which mercury propellant flow rates were calculated to be 1.2, 3.7, and 7.8 grams per hour, respectively. Figure 2 shows a schematic drawing of the thrustor along with its power supplies and parameter readouts. The thrustor was vertically mounted under a stainless-steel bell jar at the top of the vacuum chamber. A sketch showing the major components of the system is presented in figure 3.

A plasma probe was used in the tests to ascertain the extent of beam spreading. The probe consisted of 11 molybdenum current collectors spaced 3.8 centimeters apart on a rake. The rake was located 30 centimeters below the thrustor and pivoted about a point 24 centimeters from the centerline of the thrustor. A description of this type of probe can be found in reference 5. A typical profile is shown in figure 4. The profiles did not vary significantly throughout the tests.

Ion beam current was measured by an ammeter in the ground return line of the ion thrustor. Pressure was measured by a Bayard-Alpert ionization gage mounted on the inside wall of the condenser and 45 centimeters below the top of the condenser. The gage was oriented to measure pressure transverse to the beam. A second gage was located in one of the top ports of the vacuum tank. This gage was used for monitoring purposes

only. The relative positions of the gages can be seen in figure 3.

Operation was started by pumping down the vacuum system and cooling the condenser. When the pressure appeared to stabilize, the mercury boiler of the ion thrustor was turned on. As the mercury was heated, a sharp pressure rise was followed by a gradual pressure decrease. The thrustor was then heated, and when the pressure appeared to stabilize, the thrustor was operated. Various combinations of ion beam current and accelerating potential were set. When stable operation of the ion thrustor was obtained, pressure readings were taken.

The variation of pressure with time for a typical run is shown in figure 5. To determine the pressure rise, a background pressure was determined and then subtracted from the pressure readings. To determine the background pressure, which is the pressure in the system in the absence of an ion beam flow, readings were taken with the thrustor heated but without beam current. This was done before and after each test point. A sudden change in background pressure is indicated in figure 5. This change, which occurred occasionally, was not felt to affect the results. In these cases the new background pressure was used as a reference to determine the pressure rise.

Before data were taken, the condensers were allowed to become mercury coated. This condition is more typical of actual operation than a clean condenser. The coating was accomplished by heating the mercury boiler and operating the ion thrustor at low power levels for a period of several hours.

RESULTS AND DISCUSSION

Curves of pressure rise against beam current are presented in figure 6 for the smooth cylindrical condenser with both the 32° and the 148° target and the honeycomb condenser with each of the two targets. The results show no significant difference in pressure rise due to the variation of target geometry.

The data points are representative of a number of accelerating potentials. The accelerating potential range for a given beam current was limited, however, by thrustor operation. As shown, the accelerating potential variation had very little effect on pressure rise because of the limited range and the fact that accelerating potential has only a second-order effect on pressure when compared with ion beam current.

The curves in figure 6 show that at a given ion beam current the pressure rise with the honeycomb condenser is about one-half that of the pressure rise with the smooth condenser. However, the honeycomb condenser has a surface area 16 times as great as the smooth condenser and on the basis of equation (3) may be expected to exhibit a pressure rise 1/16 of the pressure rise due to the smooth condenser. This discrepancy is due primarily to the fact that the effective pumping area is not the geometric area. At

the conclusion of these tests the condensers were examined and an estimate of the effective pumping area was made by visual observation of the pattern of the mercury distributed on the condensers. The estimates of the effective area as determined from visual observation were 0.4 times the geometric area for the smooth condenser and 0.1 times the geometric area for the honeycomb condenser. These estimates are not highly accurate since considerable operating time was required before a mercury distribution pattern became evident. During this time period the ion thrustor was operated under various conditions with two different targets.

Summary data are plotted in figure 7 in a form in which the intercept of the curves represents F^*. These curves are based on the estimated effective area. An examination of the curves shows that the smooth condenser yields an F^* of 0.5 and the honeycomb condenser yields an F^* of 1.0, which result in a mean value of F^* for the two condensers of 0.75. The difference in F^* between the two condensers may be attributed in part to the fact that the determination of effective area gives only an estimate, which is not highly accurate.

Also plotted in figure 7 is the average performance, based on estimated effective condensing area, of a number of condensers reported in reference 2. In this case, the plot yields a value of 0.015 for F^*, which indicates that these condensers were considerably more efficient than the condensers used in the present investigation. This difference in performance may again be due in part to the inability to accurately determine effective area. In addition, the condensers used in the present study were larger and were allowed to become mercury coated before performance data were taken, whereas the condensers in reference 2 were cleaned prior to each run.

The data of this report and of reference 2 are based on actual ionization gage readings. The gas in the system was believed to be predominantly mercury vapor, which would result in pressure gage readings two to three times higher than the true pressure.

CONCLUDING REMARKS

The pumping performance of both a smooth and a honeycomb condenser in removing exhaust vapor from a mercury ion thrustor operating in a vacuum chamber was studied. Two targets were used with each condenser. One target had an apex angle of 148°, and the other had an apex angle of 32°. No effect due to the variation in target geometry was observed.

Mercury condensation patterns indicated that about 0.4 of the smooth cylinder was effective in pumping. The estimated effective area of the honeycomb condenser was 0.1 of its geometric area with only the first 2 to 3 centimeters of the 18-centimeter-deep fins effective in pumping.

On the basis of these estimated effective areas, a mean value of F^* was determined

to be 0.75. In a similar study (ref. 2) a mean value of 0.015 for F^* was obtained, which indicated that the condensers used in this study are considerably less efficient than those previously tested. However, in the present investigation, the data were obtained with larger condensers and the condensers were allowed to become coated with mercury prior to data acquisition.

Lewis Research Center,
National Aeronautics and Space Administration,
Cleveland, Ohio, October 21, 1965.

REFERENCES

1. Mickelsen, William R.; and Childs, J. Howard: Theoretical Analysis of Ultrahigh Vacuum Condensers. Rev. Sci. Instr., vol. 29, no. 10, Oct. 1958, pp. 871-873.
2. Richley, Edward A.; and Cybulski, Ronald J.: High-Vacuum Condenser Design: Experimental Effects from Cesium and Mercury Ion Beams. NASA TN D-1217, 1962.
3. Wachman, Harold Y.: The Thermal Accommodation Coefficient: A Critical Survey. ARS J., vol. 32, no. 1, Jan. 1962, pp. 2-12.
4. Reader, Paul D.: Investigation of a 10-Centimeter-Diameter Electron-Bombardment Ion Rocket. NASA TN D-1163, 1962.
5. Kerslake, William R.: Accelerator Grid Tests on an Electron-Bombardment Ion Rocket. NASA TN D-1168, 1962.

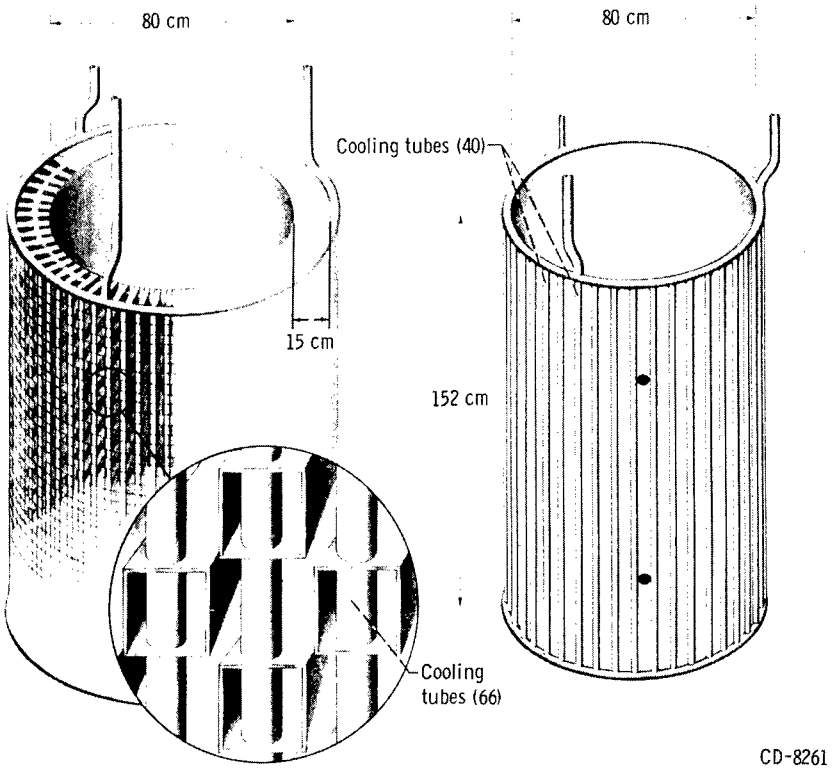

(a) Honeycomb condenser.

(b) Smooth condenser.

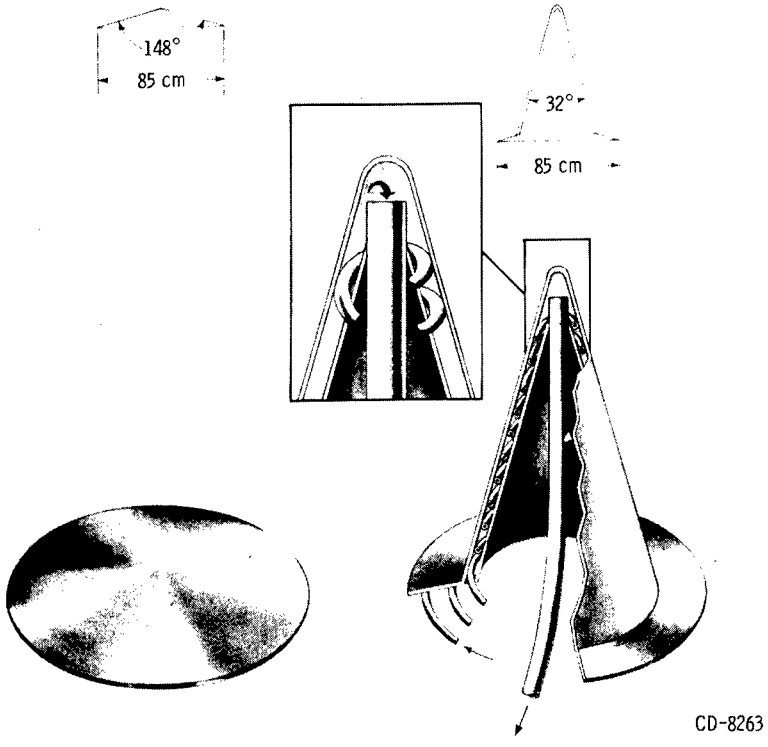

(c) 148° Target.

(d) 32° Target.

Figure 1. - Cryopump components.

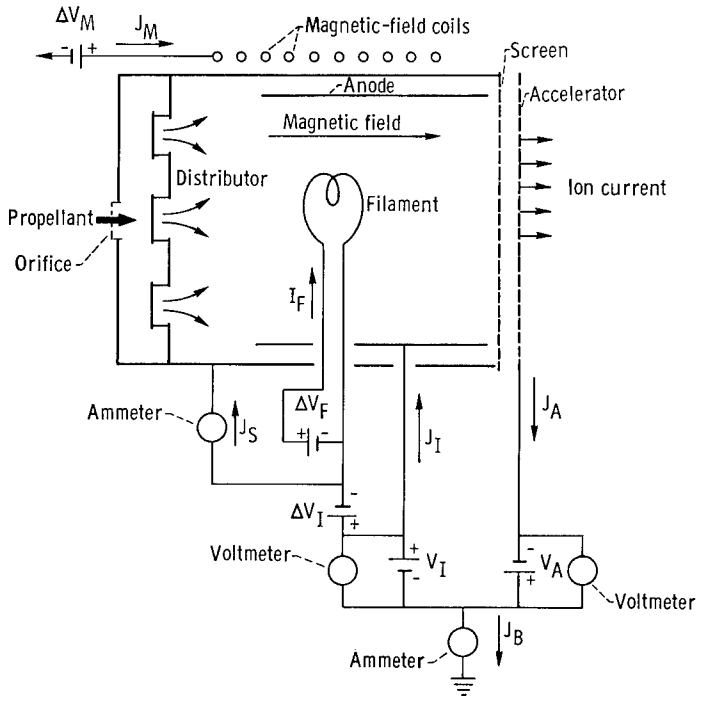

I_F filament current
J_A accelerator current
J_B beam current
J_I anode current
J_M magnetic field coil current
J_S screen current
V_A accelerator potential
V_F filament potential
V_I screen potential
V_M magnetic field coil potential

Figure 2. - Schematic of ion thrustor.

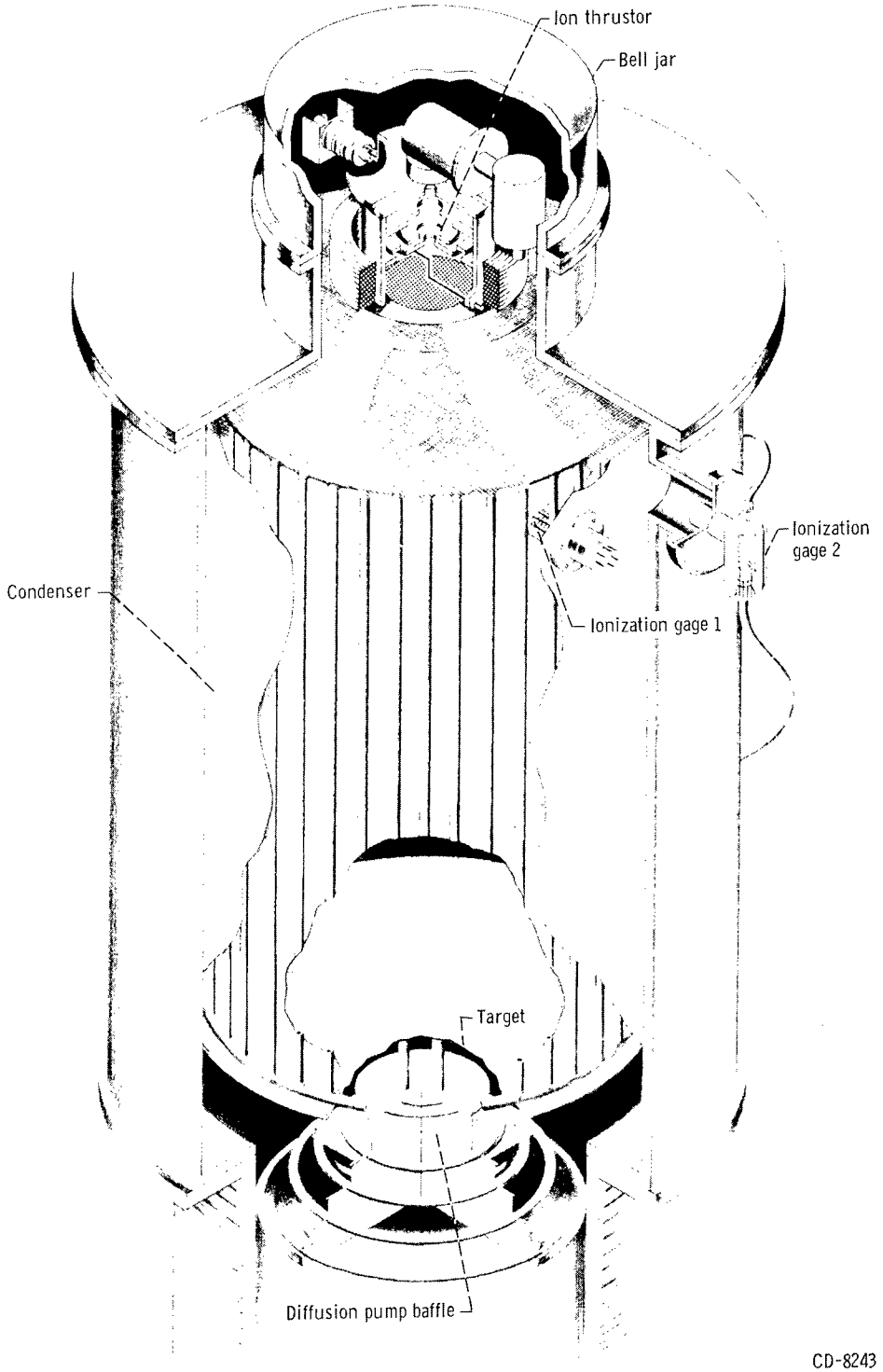

Figure 3. - Test system.

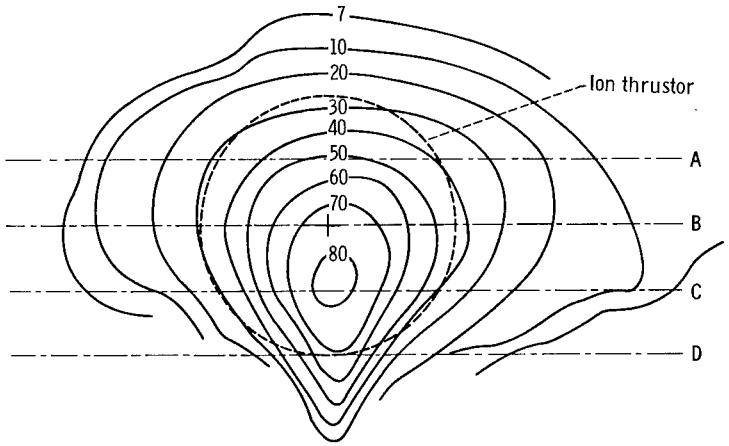

(a) Cross section of beam power density (arbitrary units).

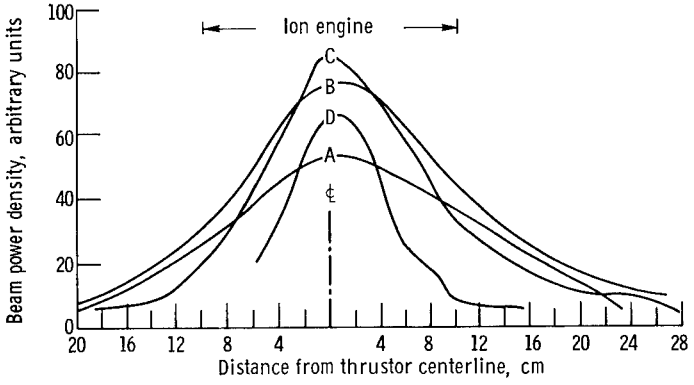

(b) Profile of beam power density.

Figure 4. - Ion thrustor beam power density distribution.

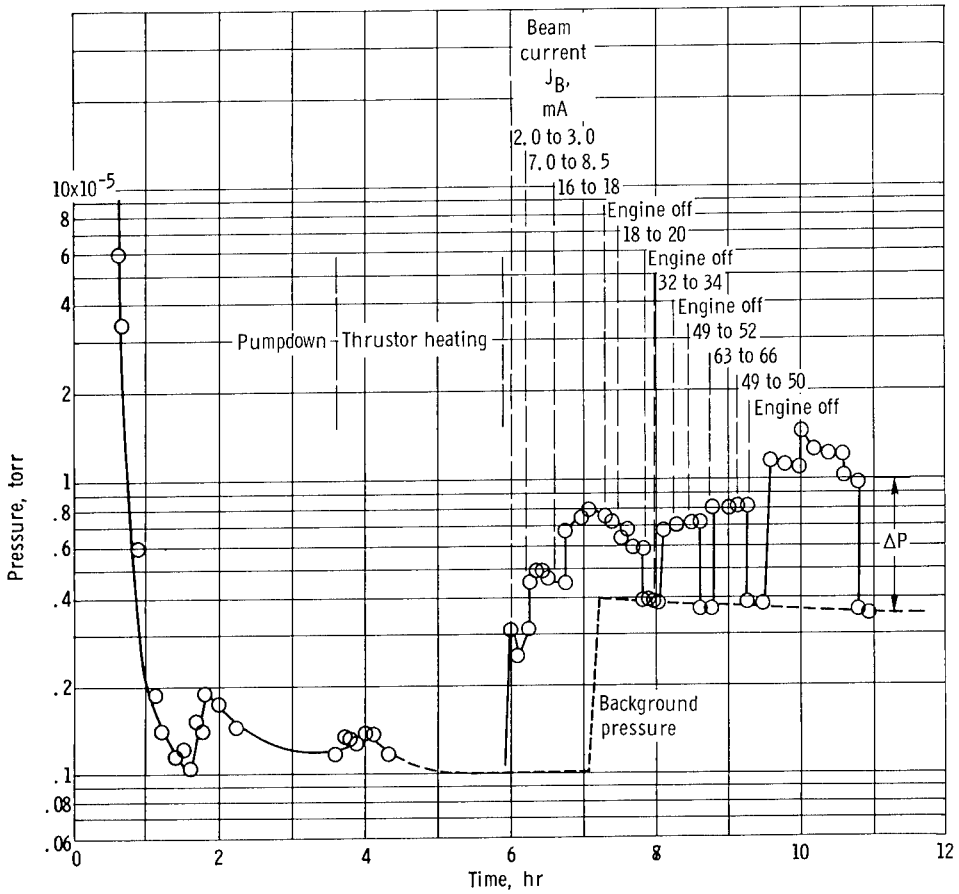

Figure 5. - Variation of pressure with time during test.

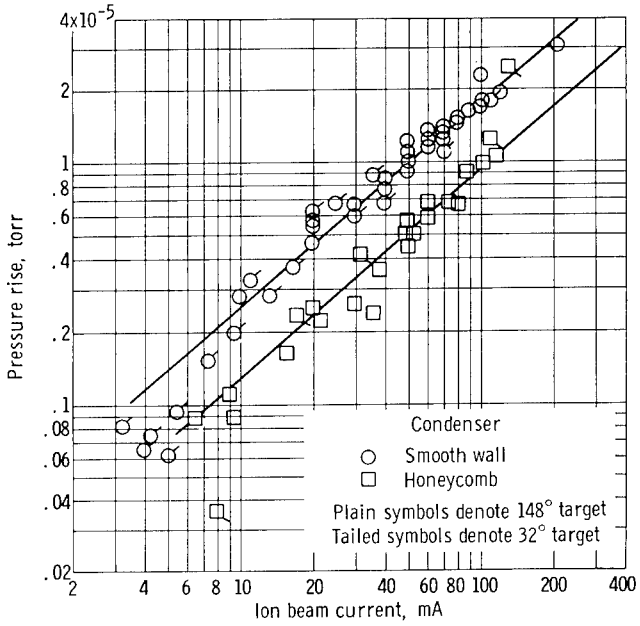

Figure 6. - Effect of ion beam current on pressure rise.

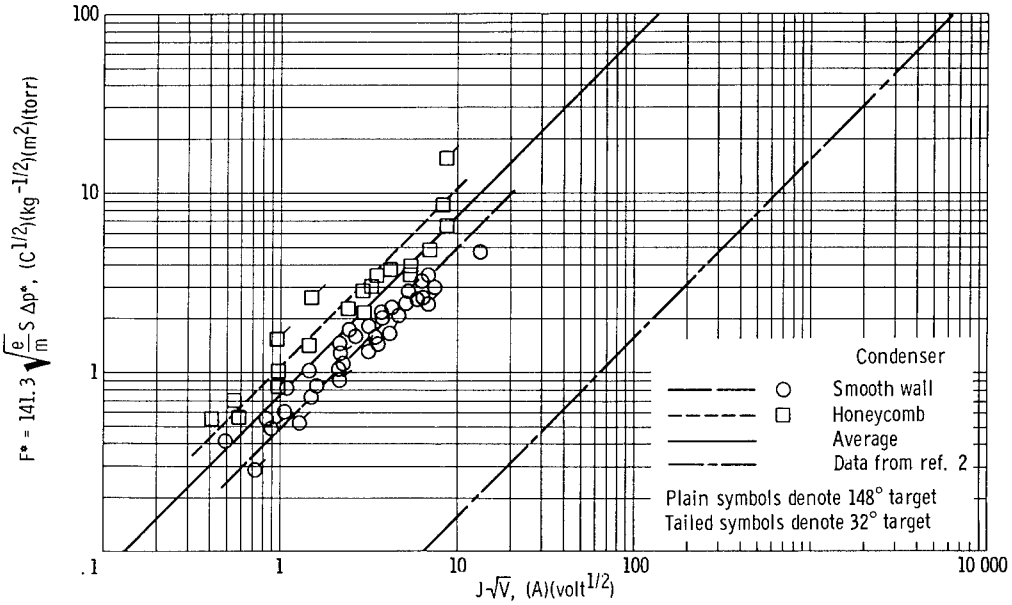

Figure 7. - Condenser performance.

"The aeronautical and space activities of the United States shall be conducted so as to contribute . . . to the expansion of human knowledge of phenomena in the atmosphere and space. The Administration shall provide for the widest practicable and appropriate dissemination of information concerning its activities and the results thereof."

—NATIONAL AERONAUTICS AND SPACE ACT OF 1958

NASA SCIENTIFIC AND TECHNICAL PUBLICATIONS

TECHNICAL REPORTS: Scientific and technical information considered important, complete, and a lasting contribution to existing knowledge.

TECHNICAL NOTES: Information less broad in scope but nevertheless of importance as a contribution to existing knowledge.

TECHNICAL MEMORANDUMS: Information receiving limited distribution because of preliminary data, security classification, or other reasons.

CONTRACTOR REPORTS: Technical information generated in connection with a NASA contract or grant and released under NASA auspices.

TECHNICAL TRANSLATIONS: Information published in a foreign language considered to merit NASA distribution in English.

TECHNICAL REPRINTS: Information derived from NASA activities and initially published in the form of journal articles.

SPECIAL PUBLICATIONS: Information derived from or of value to NASA activities but not necessarily reporting the results of individual NASA-programmed scientific efforts. Publications include conference proceedings, monographs, data compilations, handbooks, sourcebooks, and special bibliographies.

Details on the availability of these publications may be obtained from:

SCIENTIFIC AND TECHNICAL INFORMATION DIVISION

NATIONAL AERONAUTICS AND SPACE ADMINISTRATION

Washington, D.C. 20546